



**HAL**  
open science

# Quantification of tributaries contributions using a confluence-based sediment fingerprinting approach in the Canche river watershed (France)

Edouard Patault, Claire Alary, Christine Franke, Nor-Edine Abriak

► **To cite this version:**

Edouard Patault, Claire Alary, Christine Franke, Nor-Edine Abriak. Quantification of tributaries contributions using a confluence-based sediment fingerprinting approach in the Canche river watershed (France). *Science of the Total Environment*, 2019, 668, pp.457-469. 10.1016/j.scitotenv.2019.02.458 . hal-02062245

**HAL Id: hal-02062245**

**<https://hal.science/hal-02062245v1>**

Submitted on 22 Oct 2021

**HAL** is a multi-disciplinary open access archive for the deposit and dissemination of scientific research documents, whether they are published or not. The documents may come from teaching and research institutions in France or abroad, or from public or private research centers.

L'archive ouverte pluridisciplinaire **HAL**, est destinée au dépôt et à la diffusion de documents scientifiques de niveau recherche, publiés ou non, émanant des établissements d'enseignement et de recherche français ou étrangers, des laboratoires publics ou privés.



Distributed under a Creative Commons Attribution - NonCommercial 4.0 International License

## **Quantification of tributaries contributions using a confluence-based sediment fingerprinting approach in the Canche river watershed (France).**

Edouard Patault<sup>a,b,\*</sup>, Claire Alary<sup>a</sup>, Christine Franke<sup>b</sup>, Nor-Edine Abriak<sup>a</sup>

<sup>a</sup>IMT Lille Douai, Univ. Lille, EA 4515 - LGCgE - Civil Engineering and Environmental Department, F-59000 Lille, France

<sup>b</sup>MINES ParisTech, PSL Research University, Center of Geosciences, 35 rue Saint-Honoré, 77305 Fontainebleau Cedex, France

*\*Now at: Normandie Univ, Rouen, UNIROUEN, UNICAEN, CNRS, M2C, FED-SCALE, Rouen, France*

*E-mail address: [edouard.patault@imt-lille-douai.fr](mailto:edouard.patault@imt-lille-douai.fr) / [edouard.patault1@univ-rouen.fr](mailto:edouard.patault1@univ-rouen.fr) (E.Patault)*

## **Abstract**

Since a few years, land use management aims to reduce and control water erosion processes in watersheds but there is a lack of quantitative information on the contribution of the sources of transported sediment. This is most important in agricultural areas where soils are sensitive to erosion. The geology of these areas is often characterized by large expanses of relatively homogeneous quaternary silts. The possibility of distinguishing the sources of erosion according to their geological substratum is thus very delicate. This information is important because its lack can lead to the mis-implementation of erosion control measures. To address this request, a confluence-based sediment fingerprinting approach was developed on the Canche river watershed (1274 km<sup>2</sup>; northern France), located in the European loess belt, an area that is affected by diffuse and concentrate erosion processes. Suspended particulate matter was collected during five seasonal sampling campaigns using sediment traps at the outlet of each tributary and confluence with the main stream of the Canche river. The final composite fingerprint was defined using physico-chemical and statistical analyses. The best tracer parameters for each tributary were selected using stepwise discriminant function analyses. These parameters were introduced into a mass balance mixing model incorporating Monte-Carlo simulations to represent the uncertainty. Estimates of the overall mean contributions from each tributary were quantified at different temporal scales. The annual sediment flux tributaries contributions range from 3 to 22% at the outlet of the Canche river, and annual sediment flux range from 0.87 to 40.7 kt yr<sup>-1</sup>. The Planquette and the Créquoise tributaries appear to be those producing the largest sediment flux. In contrast, tributaries with the highest number of erosion control on their area exhibit the lowest values of sediment flux. Our results indicate a positive impact of recent land management policies in the Canche river watershed.

*Keywords:* sediment fingerprinting; physico-chemical tracers; tributaries; mixing model; watershed management; Northern France

## 1 **1. Introduction**

2 Information on the origin of sediment transfer in river systems is essential for watershed  
3 management. This is a complex task considering that suspended material may come from different  
4 diffuse sources and their contribution may vary over time and space as a consequence of varying  
5 erosion processes (Haddadchi et al., 2013). Indirect approaches exist to identify sediment sources  
6 (field surveys, river monitoring) but they are hampered by spatial and temporal sampling problems  
7 (Collins & Walling, 2002). Since several years, direct approaches such as the “sediment  
8 fingerprinting” method (e.g. Walling & Woodward, 1992; Collins et al., 2001; Krein et al., 2003;  
9 Motha et al., 2004; Martínez-Carreras et al., 2010; Evrard et al., 2011; Lamba et al., 2015) have been  
10 commonly applied. These approaches attempt to quantify the contributions of sediment sources at  
11 variable spatial scales: from the river section to the catchment scale. The procedure consists on the  
12 characterization of the potential sediment sources by a comparison of their bio-geo-physico-chemical  
13 properties to the transported fluvial material. The properties that have been used in previous  
14 research include sediment color (e.g. Krein et al., 2003; Poulenard et al., 2009; Martínez-Carreras et  
15 al., 2010), magnetic properties (e.g. Russell et al., 2001; Motha et al., 2004), chemical composition  
16 (e.g. Collins et al., 1997; Carter et al., 2003; Collins et al., 2012; Theuring et al., 2015), environmental  
17 radionuclides (e.g. Evrard et al., 2013; Du & Walling, 2016; Le Gall et al., 2016), and particle size (e.g.  
18 Krein et al., 2003).

19 There is a consensus that the use of a single parameter is not sufficient, and that a  
20 combination of tracers must be used to identify sediment sources (Walling et al., 1993; Collins and  
21 Walling, 2002). Because of the heterogeneity of catchments, a large panel of tracers and statistical  
22 methods to identify the best combination of parameters that discriminates the sediment sources are  
23 generally used (e.g. Collins et al., 1997; Collins et al., 2012; Palazón et al., 2015; Nosrati et al., 2018).  
24 Selected data is injected in a mixing model to quantify the contribution of each source to the target  
25 sediment. The literature describes different mathematical form of mixing models: e.g. the modified  
26 Collins model algorithm, the Hughes mixing model, the Landwehr model (Collins et al., 1997; Motha

27 et al., 2003; Hughes et al., 2009; Collins et al., 2010; Devereux et al., 2010; Gellis and Walling, 2011;  
28 Haddadchi et al., 2013). Uncertainties associated to the results of the mixing model are evaluated  
29 using mathematical algorithms. In studies dealing with the sediment fingerprinting approach,  
30 machine learning algorithms are often applied such as the Bayesian mixing model (Nosrati et al.,  
31 2018), Monte-Carlo simulations (Hughes et al., 2009; Lamba et al., 2015; Vale et al., 2016; Pulley and  
32 Collins, 2018), classification and regression trees (CART model; Choubin et al., 2018).

33 While the sediment fingerprinting method has largely contributed to the quantification of  
34 sources of sediment input for different watersheds around the world, recent discoveries showed that  
35 some scientific questions still need to be resolved (e.g. Smith et al., 2015). Some studies have shown  
36 that the selection of sources and sediment targets in a catchment may have important implications  
37 for the interpretation of the results : highly erodible areas may have a disproportionate effect on  
38 tracer concentrations (Wilkinson et al., 2013) and nearby sources may have larger contributions for a  
39 given point on a river than distant sources (Haddadchi et al., 2015). It is also important to pre-identify  
40 the sources contributing to the sediment flux as an un-sampled source can strongly bias the results  
41 (Smith et al., 2015). Thus, the selection of tracers is an important issue in this approach: uncertainties  
42 in the prediction of source contributions decrease by increasing the number of trace parameters  
43 (Sherriff et al., 2015). Predicted contributions may be different depending on the choice of tracers  
44 (Pulley et al., 2015). The conservative behavior of tracers may also introduce bias in interpretations  
45 (Sherriff et al., 2015) therefore a careful tracer selection procedure is recommended (Kraushaar et  
46 al., 2015). The type and the structure of the mixing model may also affect the results due to different  
47 mathematical approaches (see review of Haddadchi et al., 2013; and references therein). Cooper et  
48 al. (2014) showed that the estimation of the source contributions varies up to 21% between the  
49 different models. Laceby and Olley (2015) suggested that correction factors (particle size or organic  
50 matter content) did not significantly improve the results.

51 Existing “black-box” effects related to unknown transport signatures of particles were  
52 suggested by Koiter et al. (2013) and are supported by observations published by Fryirs et al. (2013).  
53 They suggest that sedimentary transport pathways cannot be assumed to be directly connected  
54 between sources and outlets, but include barriers or buffers that disrupt sediment transfer. Recently,  
55 Li et al. (2019) show that some element concentrations and their relative contributions to the surface  
56 sediments were relevant to sediment transport processes and the related flow paths, because of  
57 their association with different types of grains. To address this challenge, the so-called “tributary  
58 tracing” or “confluence tracing” approaches were recently developed (e.g. Vale et al., 2016; Nosrati  
59 et al., 2018). The latter concept consists in the consideration of tributary upstream sediments as  
60 potential sources for downstream sediments, and this approach removes a significant proportion of  
61 the impact of potential chemical enrichment on sediments due to particle size variations (Lacey et  
62 al., 2017).

63 In the Canche river watershed in Northern France, most natural hazards are related to  
64 mudflow and flooding. Mudflow causes significant damages to infrastructure that induce high  
65 economic costs. Since 2000, environmental policies are designed to reduce erosion by runoff in the  
66 Canche river watershed by implementing hard and soft erosion control measures, such as dams,  
67 retention pools, ditches or fascines. However, so far few information is available on the evaluation of  
68 the efficiency of these environmental policies.

69 The main goal of this study is to assess the suitability of the confluence-based sediment  
70 fingerprinting approach in a relatively homogeneous environmental context and to quantify the  
71 contribution of the different tributaries draining the studied agricultural watershed. As this  
72 watershed is very sensitive to erosion processes and environmental policies try to reduce the  
73 sediment input in the Canche river, this work also proposes an application of the confluence-based  
74 sediment fingerprinting approach to evaluate the possible effect of environmental policies on  
75 erosion reduction.

## 76 2. Material & Methods

### 77 2.1 The Canche river watershed

78 The Canche river watershed (1274 km<sup>2</sup>; lat.: 50°25'53"N, long.: 2°02'24"E; Fig. 1A) is situated  
79 in the European loess belt in Northern France and is characterized by oceanic climate conditions. The  
80 mean annual temperature is 11°C and the mean annual rainfall comprises 1000 ± 150 mm. Altitudes  
81 range from 0 m at the catchment outlet to 207 m in the upstream areas and catchment slopes are  
82 commonly in the range 2-3% (Fig. 1B). The watershed is characterized by a meandriform drainage  
83 network dominated by the Canche river (88 km) and seven tributaries. The watershed drains  
84 Quaternary loess on the chalky grounds of the Seno-Turonian.

85 The Canche river watershed is dominated by agricultural land use, consisting of 80% arable  
86 lands (Fig. 1C). The watershed is affected by mudflows, mainly due to diffuse and concentrate  
87 erosion on arable lands that induce an important economic cost for the local communities (Patault,  
88 2018). Moreover, surface soils are affected by water erosion leading to a highly variable specific  
89 sediment yield at the outlet of the river. The annual sediment export ranged from 29 to 185 kt  
90 between 1999 and 2016 according to the local water agency (Agence de l'Eau Artois-Picardie, 2016).

91 The mean annual discharge for the Canche river is estimated to 21 m<sup>3</sup> s<sup>-1</sup> with contributions  
92 from the following main tributaries: Ternoise (7 m<sup>3</sup> s<sup>-1</sup>), Planquette (1.5 m<sup>3</sup> s<sup>-1</sup>), Créquoise (2 m<sup>3</sup> s<sup>-1</sup>),  
93 Bras de Bronne (2 m<sup>3</sup> s<sup>-1</sup>), Course (4 m<sup>3</sup> s<sup>-1</sup>), Dordogne (2.5 m<sup>3</sup> s<sup>-1</sup>), and Huîtrepin (2 m<sup>3</sup> s<sup>-1</sup>). The flow  
94 discharge was quantified using a low-frequency monitoring station, based on water level estimations,  
95 in the Ternoise, Course, and Canche river. Flow discharge for the ungauged catchments  $Q_{ungauged}$   
96 was calculated assuming similar rainfall and hydrological regimes in the entire watershed. Values  
97 were extrapolated from the closest monitoring station by multiplying the value  $Q_{gauged}$  with the  
98 appropriate fraction related to the ratio between the closest catchment area ( $A_{ungauged}$ ) and the  
99 catchment area at the monitoring station  $A_{gauged}$  :

$$Q_{ungauged} = Q_{gauged} \times \frac{A_{ungauged}}{A_{gauged}} \quad (1)$$

100

101 with  $Q$  representing the discharge in  $\text{m}^3 \text{s}^{-1}$  and  $A$  as the area of the catchments in  $\text{km}^2$ .

102 According to Andréassian et al. (2012), this method provides robust results for ungauged  
103 catchments. Cross validation with the high-frequency monitoring station on the Canche river  
104 watershed evaluated a 17% associated error (Fig. S1).

## 105 *2.2 Sediment sampling*

106 Suspended particulate matter (SPM) were collected using sediment traps installed at each  
107 tributary outlet and each confluence with the Canche river (Fig. 1D). Sampling campaigns were  
108 conducted in winter 2015, winter 2016, spring 2016, summer 2016, and autumn 2016. A total of 65  
109 samples was collected. More details on the sampling devices, exact sampling periods, and site  
110 positions are available in Figure 2 and Table S1.

111 The samples consist of recently suspended solids transported in the different tributaries.  
112 Sediment was sampled using an experimental device adapted from previous studies (described by  
113 Tessier (2003) and Kayvantash et al. (2017)). The sediment traps (Fig. 2) consist of 2 l polyethylene  
114 bottles, perforated at 5 cm from the top with two opposite holes (diameter 5 cm). The bottle is  
115 attached to the river bank with a rope and deposited in the channel. The device is hold in place using  
116 either an additional rope or a combination of rope and a wooden beam. The whole device is  
117 weighted vertically in the water column using ballast that is adapted to the river flow speed. Traps  
118 usually captured between 50 and 100 g of sediments during ~5-7 days water expose. Recent work in  
119 the Seine river in France, observed that there is no significant grain size selection depending on the  
120 position of the bottle in the river channel (Kayvantash, 2016; Kayvantash et al., 2017).



121 *2.3 Sedimentological and geochemical analysis*

122 All samples were analyzed to obtain particle size distribution and elemental composition.  
123 Grain size analyzes were performed using a *Beckman Coulter LS 13320* laser particle sizer. All samples  
124 were initially oven-dried at 30°C for 72 h and sieved to 2 mm to remove any coarser debris, such as  
125 leafs and roots, that could distort further measurement. Two grams of sediment were mixed with  
126 100 ml of ultrapure water and were stirred during 5 min using ultrasonic dispersion to homogenize  
127 the sample. Each solution was analyzed in triplicates to validate the measurement.

128 The analysis of the elemental composition was carried out after acid mineralization in a  
129 microwave oven. 22 reactors were used for mineralization, 0.250 g of a sample were injected in 18  
130 reactors, 2 reactors are used as references with TH2 (reference sediment material) to test the validity  
131 of the analysis by comparison with referenced measurements, and 2 blank reactors (without addition  
132 of solid material) are used to ensure non-contamination during preparation. For each reactor, 1 ml of  
133 nitric acid (HNO<sub>3</sub>), 3 ml of hydrochloric acid (HCl), and 0.5 ml of water (H<sub>2</sub>O) is added to the sediment.  
134 The determination of the major elements in the liquid phase (Al, Ca, Fe, K, Mg, Mn, Na, P, S, Si, Sr, Ti,  
135 Zn) was performed using an inductively coupled plasma atomic emission spectrometer (ICP-AES; *ICAP*  
136 *7400 Thermo Fischer Scientific*). The determination of the trace elements (As, Ba, Bi, Cd, Ce, Co, Cs,  
137 Cr, Cu, La, Li, Mo, Ni, Pb, Rb, Sb, Sc, Se, Sn, Th, Tl, U, V) in the samples was carried out using an  
138 inductively coupled plasma mass spectrometer (ICP-MS; *PerkinElmer NexION 300x*).

139 *2.4 Sediment fingerprinting procedure*

140 Several analytical and statistical steps were used, using the model *Sed\_Sat-v1.0* (Gorman  
141 Sanisaca et al., 2017) to determine which tracers are most significant in defining tributaries and  
142 quantifying the relative contributions of tributaries to the suspended sediment samples. The model is  
143 written using the statistical software *R* (R Core Team, 2013) and *Microsoft Access*® is used as a user  
144 interface.

145 *2.4.1 Test for univariate normal distribution*

146           The following procedure of the Sed\_Sat-v1.0 model assumes normality among the analyzed  
147 variables. As a first step of the model, all variables were tested for normality, using the Shapiro-Wilk  
148 test (Shapiro and Wilk, 1965), to determine if the raw concentration values are normally distributed  
149 within each source group. All variables that were not normally distributed were tested again for  
150 normality after transformation using the Tukey Ladder of Powers transformations (Table S2; Tukey,  
151 1977).

#### 152 2.4.2 Outlier test

153           The average and the standard deviation within each source group for each tracer were  
154 determined. If the tracer value for a given source sample exceeded three times the standard  
155 deviation of the average value, the sample was considered an outlier and removed from the tracer  
156 set (Wainer, 1976; in Gellis et al., 2013).

#### 157 2.4.3 Range test

158           A condition for sediment fingerprinting is that the tracer concentration values in the target  
159 dataset must be conservative and do not change during transport (Walling et al., 2002). A range test  
160 was used to determine if for any given tracer, the target samples lie within the range of the tracer  
161 concentration values in the source dataset. Any tracers that fail to satisfy this condition within the  
162 measurement error (10% of each fluvial sample's tracer value) are considered non-conservative and  
163 were removed from dataset (Gellis et al., 2013; Gorman Sanisaca et al., 2017).

#### 164 2.4.4 Stepwise Linear Discriminant Function Analysis (DFA)

165           To create the final group of tracers that differentiate the tributaries, a stepwise linear  
166 discriminant function analysis (DFA) was performed. The stepwise linear DFA identifies tracers that  
167 yield the greatest separation between the tributaries and rejects variables that do not contribute  
168 based on the minimization of the Wilk's lambda criterion. The closer the Wilk's lambda statistic is to

169 zero, the more significant a tracer's contribution is to the linear discriminant function. The model  
170 selects a combination of tracers that provide optimal separation.

#### 171 2.4.5 Mixing model

172 The remaining set of tracers selected in the stepwise DFA is incorporated into a mixing model  
173 to estimate the relative proportion of the sediment source to the target sample. The mixing model  
174 was developed and used by Collins et al. (2010). The model uses a set of linear equations for each  
175 composite signature by minimizing the sum of squares of the weighted relative errors according to  
176 Eq. 2:

$$\sum_{i=1}^n \{ [C_i - (\sum_{s=1}^m P_s S_i)] / C_i \}^2 W_i \quad (2)$$

177

178 Where  $C_i$  is the concentration of tracer  $i$  in the target sample;  $P_s$  is the optimized percentage  
179 of contribution source type ( $s$ );  $S_i$  is the mean concentration of tracer  $i$  in source  $s$ ;  $W_i$  is the  
180 weighting factor for tracer  $i$ ;  $n$  is the number of tracers comprising the optimum composite  
181 fingerprint; and  $m$  is the number of sediment source types.

182 The model adheres to two constraints that must be satisfied to produce realistic values,  
183 which are: each source group proportion is constrain to a positive value between 0 and 1, and is  
184 expressed as:

$$0 \leq P_s \leq 1 \quad (3)$$

185 And the sum of all source group contributions has to be equal to 1 and is expressed as:

$$\sum_{s=1}^m P_s = 1 \quad (4)$$

186

187           The tracer discriminatory weighting value,  $W_i$ , is used to reflect the tracer discriminatory  
188 power, based on the relative discriminatory power of each individual tracer provided by the results  
189 of the stepwise DFA. The weighted values ensure that tracers with higher discriminatory power are  
190 optimized in the mixing model. The weighting for each tracer that passed the stepwise DFA is  
191 calculated as follows:

$$W_i = \frac{P_i}{P_{opt}} \quad (5)$$

192

193   Where  $P_i$  is the percentage of correctly classified source samples using tracer  $i$  and  $P_{opt}$  is the  
194 percentage of correctly classified source samples using tracer with the lowest  $P_i$ .

195           Tributaries relative contributions were determined for each sample at each confluence with  
196 the Canche river. Tributaries percentages are presented for each sampling campaign and were also  
197 used to quantify the sediment yield of each tributary.

198 2.4.7 Monte-Carlo simulations and virtual sample mixtures

199 Monte-Carlo simulations were used to evaluate the uncertainties in the confluence-based  
200 sediment fingerprinting results produced by the mixing model. The Monte-Carlo simulation randomly  
201 removes one sample from each of the eight source type groups and the mixing model is run without  
202 these samples. The Monte-Carlo simulation is run 1,000 times on each fluvial sample (Gellis et al.,  
203 2015). For each of the 1,000 iterations, the minimum-maximum, and the average sediment source  
204 for each tributary are determined. The robustness of the final set of tributaries and tracers is defined  
205 using the difference between the final mixing model results, the average, the minimum and  
206 maximum source percentage results produced by the Monte-Carlo simulation (Gellis et al., 2013).

207 Virtual sample mixtures are commonly used to assess if mixing model results provide an  
208 acceptable range of uncertainty (Haddadchi et al., 2014; Palazón et al., 2015; Pulley and Collins,  
209 2018). Thus, we test the robustness of the employed mixing model using tracer values of virtual  
210 sample mixtures. These virtual samples consists in hypothetical sediment provenance of equal input  
211 from each tributary, and subsequently were mathematically calculated at each confluence. The  
212 hypothetical composition of the virtual sample mixtures were then compared to the un-mixed  
213 composition calculated by the model. The accuracy of the modelling approach was tested based on  
214 the Mean Absolute Error (MAE) at each confluence:

$$MAE = \frac{\sum_{j=1}^m |X_j - Y_j|}{m} \quad (6)$$

215 Where  $X_j$  is the hypothetical percentage of each source ( $j$ ) in mixtures sediments,  $Y_j$  is the  
216 calculated contribution of each source and  $m$  is the number of sources ( $m = 8$ ).

217 2.5 Efficiency of erosion control measures

218 Information on the locations of erosion control measures (runoff retention pools, check  
219 dams, fascine, etc.) in the Canche river watershed were provided by the Chamber of Agriculture  
220 using the Database *RUISSOL* (Chambre d'Agriculture Nord-Pas-de-Calais, 2013). For each tributary,

221 the number of erosion control measure was extracted. We empirically defined an Erosion Control  
222 Index,  $ECI_i$ , using the number of erosion control measures installed on each catchment divided by  
223 their respective area:

$$ECI_i = \frac{\sum_1^n ECM_i}{A_i} \quad (7)$$

224

225 With  $ECM_i$  presenting the number of erosion control measures installed on the catchment  $i$ ;  
226 and  $A_i$  as the area of the catchment  $i$  in  $\text{km}^2$ .  $ECI_i$  was then compared to the annual tributary  
227 sediment yield (in kt) calculated using the mixing model and Monte-Carlo simulations.

### 228 **3. Results**

#### 229 *3.1 Sediment analysis*

230 The particles size analysis highlights the absence of significant differences between the D50  
231 (median particle size) of the tributaries ( $60.3 \pm 6.7 \mu\text{m}$ ) in comparison to the sediment sampled at  
232 each confluence in the Canche river ( $67.9 \pm 10 \mu\text{m}$ ; Fig. 3). A t-test between the tributaries and the  
233 confluences did not show any significant difference between their D50 ( $p\text{-value} = 0.107$ ). Thus for  
234 further model analyses, no particle size correction was applied considering that no significant particle  
235 size effect affects the direct comparison between tributaries and confluences samples.

236 The geochemical analysis showed evidence of some element concentration heterogeneities  
237 for the different sources (Fig. 4). The range of element concentrations is particularly high for some  
238 major elements (Ca:  $22054.9 - 42314 \mu\text{g g}^{-1}$ ; S:  $1013.4 - 4723.3 \mu\text{g g}^{-1}$ ) and trace elements (Ce:  $29.4 -$   
239  $55 \mu\text{g g}^{-1}$ ; La  $16.6 - 30.7 \mu\text{g g}^{-1}$ ). The element concentrations for the confluences are generally in the  
240 range of the values observed for the tributaries. Sometimes the range of the values for confluences is  
241 higher than the range for tributaries (Bi, Ca, Cu, Na, and Sr). Even though the Canche river catchment  
242 exhibits a homogeneous geology, major and trace elements seem to have a non-negligible potential  
243 for discriminating sources and quantify their contribution to the suspended sediment sampled at

244 each confluence. Considering this first approach, robust statistical analyses are needed to explore the  
245 entire dataset.

### 246 *3.2 Final composite fingerprint*

247 The first analysis consisted in the identification of outliers in the source dataset. Results  
248 showed no outliers for any tributary. Thus, all tracer parameters were kept for further analysis.  
249 Table S3 presents the results of the bracket test and shows that different elements were considered  
250 conservative at each sub-basin outlet (spatial sediment sources). Tracers were considered  
251 conservative when, for any given tracer, no significant changes during transport between upstream  
252 sources and downstream sediment sampling sites occurred. At each confluence, more than twenty  
253 tracers were considered conservative and kept for further analysis except for the confluence C2  
254 where only nine tracers were considered conservative. Cross validation using bi-plots of tracers of  
255 tributary and confluence samples confirmed the conservativeness/non-conservativeness of these  
256 tracers (Fig.S2). For the pairs of tracers that are significantly correlated ( $R^2 > 0.8$ ) within the tributary  
257 sample dataset, the correlation is maintained when adding the confluence dataset suggesting a high  
258 degree of conservatism. For other tracer pairs, the correlation is not maintained when adding the  
259 confluence sediment samples, which suggests a non-conservative behaviour. These tracers were  
260 correctly identified by the range test and were removed from further analysis.

261 With the remaining set of tracers, the stepwise DFA produced a final composite fingerprint at  
262 each confluence that provides sources discrimination (Table 2). The final composite fingerprint  
263 includes different chemical tracers that minimizes the Wilk's lambda criterion and that maximizes the  
264 source sample discrimination. At each confluence, the proposed final composite fingerprint correctly  
265 classified between 53 and 100% of the source samples in their correct affiliation. The classification is  
266 better for the confluence C1, C3, and C4, reaching values from 69 to 100%. Chemical tracers selected  
267 for the different final composite fingerprint principally include transition metals (44%), metalloids  
268 and alkaline earth metals (32%), and other element classes (24%; alkali metals, nonmetals,

269 lanthanides and actinides). Selected tracers are appropriate, considering the geochemical  
270 background level of the Canche watershed and the point or non-point discharges mainly induced by  
271 agricultural activity.

### 272 *3.3 Monte-Carlo simulations*

273 The range of Monte-Carlo simulations results show difference of  $\pm 10\%$  in comparison with  
274 the average resulting from the mixing model (Fig.S3). The relative contributions calculated by the  
275 mixing model at each confluence are considered robust, despite a large spread of the Monte-Carlo  
276 results between minimum and maximum values can be observed for some confluences (C2 - C5).  
277 Nevertheless, the increase of sources, after confluence C5, tends to decrease the uncertainties in the  
278 Monte-Carlo simulations.

279 Modelling results using virtual mixtures at each confluence confirm that all sources are well  
280 recognized by the mixing model (Fig.5). The MAE values are relatively low and are thus considered  
281 acceptable, ranging from 0.93 to 6.36%, with a slight variability within each confluence (min = 0.27  
282 and max = 7.57%). The results are considered robust, even with a high number of sources at the last  
283 confluence (m = 8 and MAE = 2.1%). This test supports the hypothesis that the applied methodology  
284 is reliable.

### 285 *3.4 Annual tributaries contributions*

286 Annual tributaries relative contributions could be calculated using the four campaigns  
287 performed during the year 2016 (Fig. 6). The results show in general a high and persistent relative  
288 contribution of the Planquette and the Créquoise along the main channel. For example, the relative  
289 contribution of the Planquette at point C3 is 19% and 21% at point C7. The contributions of the  
290 upstream part of the Canche river and the Ternoise are particularly high in the upstream areas (33  
291 and 49% at point C2) but tend to decrease as we approach the outlet of the catchment (12 and 3% at  
292 point C7). The relative contribution of the Course seems important in the downstream area except  
293 for the point C6 that may have encountered a mis-classification of the source samples (C5: 24% -; C6:



294 3%; C7: 15%). The relative contributions of the downstream tributaries (Dordogne and Huîtrepin) are  
295 generally moderate as their outlet is closer to the sampling point. These average results over four  
296 sampling campaigns corresponding to the hydrologic year 2016 seem consistent if we consider the  
297 relative hydrological contributions of each tributary to the Canche main stream and the length of the  
298 main channel. Spatial variations show that along the Canche river catchment, the sedimentary  
299 signatures of the upstream tributaries tend to decrease as we approach the downstream indicating a  
300 possible effect of storage and/or dilution of the sediment flux.

### 301 *3.5 Tributaries sediment yield*

302 Considering the information provided by the Artois-Picardie Water Agency, the annual  
303 sediment yield of the Canche river catchment ranges from 29 to 185 kt yr<sup>-1</sup> since 1999. The relative  
304 contributions were previously evaluated at point C7 as follows: Canche 12%, Ternoise 3%, Planquette  
305 22%, Créquoise 20%, Bras de Bronne 7%, Course 15%, Dordogne 6%, and Huîtrepin 15%. Based on  
306 the lower and upper boundaries of the annual sediment yield, the range of the sediment yield and  
307 specific sediment yield from tributaries to the main stream were calculated (Table S3). The highest  
308 sediment yields were calculated for the Créquoise and the Planquette, 5.8 – 37 kt yr<sup>-1</sup> and  
309 respectively 6.38 – 40.7 kt yr<sup>-1</sup>. The lowest sediment yields were estimated for the Ternoise (0.87 –  
310 5.55 kt yr<sup>-1</sup>), the Bras de Bronne (2.03 – 12.95 kt yr<sup>-1</sup>), and the Dordogne (1.74 – 11.1 kt yr<sup>-1</sup>).

### 311 *3.6 Impact of erosion control measures*

312 Considering that catchment stakeholders implemented 1590 erosion control measures in the  
313 Canche river watershed since 2000, this study proposes to evaluate their efficiency using the defined  
314 erosion control index ( $ECI_i$ ) and the sediment yield of each tributary previously calculated. Here, we  
315 solely implement the total number of the measures installed, as considered parameter in the  $ECI_i$ .  
316 We precise that there exist several types of erosion control measures in the field (fascines, grass  
317 strips, hedges, ponds, dams, nozzles, ditches). Nevertheless, the ratio between the different types of  
318 measures is similar whatever the treated catchment. Our results show a positive impact of the

319 installation of erosion control measures. Catchments characterized by flow discharge around  $1 \text{ m}^3 \text{ s}^{-1}$   
320 with the highest  $ECI_i$  (Dordogne, Bras de Bronne, Huîtrepin) exhibit low values of sediment yield  
321 (Fig. 7). For catchments with similar fluxes and for which few erosion control measures were installed  
322 so far (Créquoise, Planquette, Course), high values of sediment yield are observed. The relation  
323 between sediment yield and  $ECI_i$  decreases as the number of erosion control measures increases on  
324 a catchment. These results are consistent with the environmental policies of the last decades and  
325 confirm their benefits. The upstream and middle catchments all present a low  $ECI_i$  ( $\sim 1$ ). The  
326 upstream Canche and Ternoise catchments characterized by large areas show a high flow discharge.  
327 Surprisingly the suspended matter flux is much lower than for the other catchments. It is suggested  
328 that large catchment areas with high flow discharge are also those where the proportion of erosion-  
329 sensitive surfaces is lower than for small catchments. We also assume a preferential deposit of their  
330 sediment contribution in the upstream part of their respective river channel.

### 331 *3.7 Seasonal variability of tributaries contributions*

332 The seasonal contribution of each tributary at each confluence was estimated for the five  
333 sampling campaigns (Fig. 6). An important seasonal variability can be observed along with major  
334 fluctuations in relative source contributions. In general, we can observe an important relative  
335 contribution of the upstream tributaries (Canche upstream, Ternoise, Planquette, and Créquoise).  
336 The downstream tributaries (Bras de Bronne, Course, Dordogne, and Huîtrepin) exhibit lower  
337 contributions to the sediment yield except for the Bras de Bronne in winter 2015 and summer 2016,  
338 and for the Course in winter and spring 2016. For the upstream tributaries, the influence of the  
339 Planquette is more effective in dry seasons: summer and spring 2016, the influence of the Créquoise  
340 is more effective during wet seasons: winter and autumn 2016. The relative contribution of the  
341 Canche is more pronounced during winter and spring 2016 whereas for the Ternoise, the relative  
342 contribution is greater in summer and autumn 2016. An effect of storage and/or dilution can be  
343 easily observed along the main channel of the Canche river. The relative contributions of the  
344 upstream catchments generally decrease when approaching of the downstream sections. Moreover,

345 relative contributions of some downstream tributaries, such as the Dordogne or the Bras de Bronne,  
346 generally decrease near the sampling point (outlet of the respective tributary).

## 347 **4. Discussion**

### 348 *4.1 Meaningful implications for erosion control strategies*

349 The quantification of the tributaries relative contributions using a confluence-based  
350 sediment fingerprinting approach was quite conclusive, even in this relatively homogeneous  
351 lithological context comprising silty soils which as highly sensitive to erosion processes. The sampling  
352 strategy deployed was original and spatially representative of the catchment, following the need for  
353 robust sediment fingerprinting approaches as stated by several authors (Smith et al., 2015; Laceby et  
354 al., 2017). This approach was based on a relatively simple but effective field methodology on selected  
355 strategic sampling points, collecting suspended particulate matter with sediment traps in the Canche  
356 watershed at each tributary and each confluence. Time-integrated sediment traps have appeared as  
357 very suitable experimental devices to sample a large amount of suspended sediment matter during a  
358 restricted sampling period and to study sediment fluxes fluctuations. As stated e.g. by Phillips et al.  
359 (2000), Russell et al. (2000), or recent sediment fingerprinting studies on suspended sediment by e.g.  
360 Huisman et al. (2013) and Lamba et al. (2015), the use of comparable time-integrated sampling  
361 devices is much more representative for this kind of study than point sampling. According to Walling  
362 and Webb (1987), sediment transport is highly episodic (90% of annual load is transported within  
363 only 10% of the time).

364 The confluence-based approach developed in this study was also particularly effective. As  
365 emphasized by Vale et al. (2016), the short distance between upstream and downstream sediment  
366 samples limits the effect that non-conservative behavior has on geochemical signature uncertainties.  
367 The use of geochemical tracers was relevant in the Canche river watershed, even regarding the  
368 homogeneous lithological context, because of significant element composition differences between  
369 the tributaries. Differences are assumed to be mainly driven by lithological background level and the

370 point or non-point discharge induced by agricultural activities. The results of the simulations showed  
371 that tributaries located in the central part of the Canche river watershed (Planquette, Créquoise)  
372 were the most contributing to the sediment yield. They also highlight contrasted responses from one  
373 season to another, certainly in relation to rains entailing erosive event, which concern in a short  
374 time, a localized area.

375 This work provided conclusions to estimate the spatial evolution of erosive dynamics over a  
376 considerably wide area, particularly in relation to the development plans of erosion control facilities.  
377 These methodologies can successfully locate the most contributing areas in term of erosion. The  
378 results of the study also showed that the environmental policies of the last decades in Northern  
379 France seem effective, confirming the recent observations made by Frankl et al. (2017). For  
380 catchments with similar areas and fluxes, those with the less erosion control measures installed,  
381 exhibit the highest relative contributions to the sediment yield. To our knowledge, this study is the  
382 first one comparing results from a confluence-based sediment fingerprinting approach to the land  
383 management policies on a watershed. The results are significant, particularly in the given  
384 homogeneous context, which enhances the novelty of the approach and thus should be tested for  
385 other environmental contexts taking into account the specificities of the studied catchment.

#### 386 *4.2 Limitations and uncertainties*

387 The tributaries contributions quantified in this study using the confluence-based sediment  
388 fingerprinting approach must be interpreted in the context of some limitations and uncertainties.  
389 The target river sediment for source apportionment was collected from a single downstream location  
390 for each tributary. The estimated catchment proportions at each confluence therefore strongly relate  
391 to the respective sampling site. Koiter et al. (2013) pointed out that sources estimates are scale-  
392 dependent and can differ for sampling locations along a channel network. This limitation, the so-  
393 called “black-box”, remains one of the largest limitations of the sediment fingerprinting approach.

394 Sediment sampling also needs to be temporally representative. Our approach addresses this  
395 question with a seasonal sampling, although our tributaries estimations are representative of five  
396 weeks over two years. It is likely that multiple major flood event could have transported a significant  
397 proportion of the annual sediment load and may have not been sampled here. Automatic sediment  
398 samplers could be deployed on each key location to increase the temporal representability with the  
399 big disadvantage that much more sampling logistics would be needed. Considering these limitations,  
400 two approaches need to be explored. First, we may suggest the use of other sediment traps, which  
401 offers a larger sediment storage capacity and that can be dropped at key locations during a few  
402 months. Secondly, as suggested by Guzmán et al. (2013), we may suggest finding other tracers  
403 requiring inexpensive and rapid analysis approach to process quickly a large number of samples. This  
404 seems feasible using the spectrophotometric or magnetic tracers (Krein et al., 2003; Legout et al.,  
405 2013; Patault, 2018). They allow rapid, non-destructive and quantitative measurements of soil and  
406 sediment property.

407 Although tracer properties were tested for transformation using the range test, this does not  
408 confirm the complete absence of tracer property transformation during sediment delivery. As shown  
409 by Sherriff et al. (2015), the non-conservative behavior of a single tracer property included in a mass  
410 balance mixing model can affect the predicted source contributions. According to Zhang and Liu  
411 (2016), a more stringent statistical analysis than only the bracket test comprised in the *Sed\_Sat-v1.0*  
412 model, could be proposed to confirm the absence of non-conservative tracers using mixing polygon  
413 test. Moreover, Kraushaar et al. (2015) suggested an expanded procedure including water sample  
414 analyses to identify tracers that may be susceptible to dissolution during transport. Using the  
415 sediment traps deployed in this study, the experiment could be easily done. Further research in this  
416 way is strongly recommended.

417 Particle size effect on element concentration remains one of the biggest uncertainties in  
418 sediment fingerprinting approach. Differences between sources and downstream sediments may

419 arise from selective transport (Koiter et al., 2015). Our confluence-based approach, as shown in the  
420 work of Vale et al. (2016) and Nosrati et al. (2018), decreases the effect that particle size can exert on  
421 predicted source contributions. Our analysis proves that the median particle size (D50) was  
422 practically the same for all tributary and confluence samples, and thus no correction factor were  
423 applied. For future research, the confluence-based approach should be largely explored.

424 Virtual sample mixtures considering hypothetical tributary provenance (e.g. equal inputs)  
425 confirmed the robustness of the applied methodology. Uncertainties were relatively low, showing  
426 only slight evidence of variability within each confluence. However, virtual sample mixtures still  
427 remain hypothetical, experiments on artificial sample mixtures of known sediment proportions as  
428 suggested by Pulley and Collins (2018) would help further refine the modelling results. Also, as  
429 suggested by Pulley et al. (2015), tracer selection must maximize contrasts in tracer concentrations  
430 between all sources. In the case of the Canche river watershed, which shows a very homogeneous  
431 geology; existing but slight differences between the source tracers concentrations were observed.  
432 Considering this, we suggest increasing the number and the type of tracers by addition of more  
433 discriminating parameters related to the typology of the organic matter.

## 434 **5. Conclusions**

435 The study successfully shows that a confluence-based sediment fingerprinting approach  
436 using time-integrated samplers (sediment traps) and physico-chemical analyses on suspended  
437 sediment matter, allows discriminating the relative sediment yield contribution of the different  
438 tributaries that compose a given catchment, even in a homogeneous lithological context. Best tracers  
439 able to discriminate the tributaries (transition metals, metalloids, and alkaline earth metals) were  
440 identified using statistical analyses and were incorporated into a mass balance mixing model  
441 (*Sed\_Sat-v1.0 model*). Discriminating tracers were assumed to be mainly driven by the lithological  
442 background level and the point/non-point discharge induced by agricultural activities. Annual  
443 tributary contributions were evaluated and range from 3 to 22% at the outlet of the main stream.

444 Validation using virtual sample mixtures allow considering that the methodology presented is robust.  
445 Considering information given by the Artois-Picardie Water Agency, the annual tributary sediment  
446 delivery actually ranges from 0.87 to 40.7 kt yr<sup>-1</sup>. The Planquette and the Créquoise were considered  
447 as the most erosive tributaries of the Canche watershed. Tributaries with the highest number of  
448 installed erosion control measures on the territory exhibit the lowest values of sediment export  
449 confirming the generally positive impact of recent land management policies in Northern France. This  
450 novel approach allows to evaluate the relevance of environmental strategies to reduce water erosion  
451 in the studied watershed, and easily provides helpful information on decision support for future land  
452 management.

### 453 **Acknowledgements**

454 This work was financially supported by the Mines-Telecom Institute of Lille-Douai, with  
455 additional funding provided by the Artois-Picardie Water Agency (QUASPER project). We would also  
456 like to acknowledge technical support from the SYMCEA and the regional Chamber of Agriculture  
457 Nord-Pas-de-Calais, France. The authors are grateful to L. Alleman and B. Malet for the *ICP-MS/AES*  
458 analyses (IMT Lille-Douai – SAGE department). The authors thanks A. Gellis and L. Gorman Sanisaca  
459 (USGS) who provided the *Sed\_Sat-v1.0* model and for their helpful discussions. The authors also  
460 thanks the four anonymous reviewers who provided constructive suggestions to improve the  
461 manuscript.

### 462 **References**

- 463 Agence de l'eau Artois-Picardie. (2016). *Schéma Directeur d'Aménagement et de Gestion des Eaux du*  
464 *Bassin Artois-Picardie*. Retrieved from <http://www.eau-artois-picardie.fr/sdage>
- 465 Carter, J., Owens, P., Walling, D., & Leeks, G. (2003). Fingerprinting suspended sediment sources in a  
466 large urban river system. *The Science of The Total Environment*, 314–316(03), 513–534.  
467 [https://doi.org/10.1016/S0048-9697\(03\)00071-8](https://doi.org/10.1016/S0048-9697(03)00071-8)
- 468 Chambre d'agriculture Nord-Pas-de-Calais. (2013). RUISSOL: Outil de gestion des données liées au  
469 suivi des ouvrages de lutte contre l'érosion des sols agricoles.  
470 <https://www.ruissol.pro/CGI/DLL.dll?APP=3&MODULE=Ruissol>
- 471 Choubin, B., Darabi, H., Rahmati, O., Sajedi-Hosseini, Kløve, B. (2018). River suspended sediment  
472 modelling using the CART model: A comparative study of machine learning techniques. *Science*

- 473           of the *Total Environment*, 615, 272-281. <https://doi.org/10.1016/j.scitotenv.2017.09.293>
- 474 Collins, A. L., Walling, D. E., & Leeks, G. J. L. (1997). Use of the geochemical record preserved in  
475 floodplain deposits to reconstruct recent changes in river basin sediment sources.  
476 *Geomorphology*, 19, 151–167. [https://doi.org/10.1016/S0169-555X\(96\)00044-X](https://doi.org/10.1016/S0169-555X(96)00044-X)
- 477 Collins, A. L., Walling, D. E., Sickingabula, H. M., Leeks, G. J. L. (2001). Suspended sediment source  
478 fingerprinting in a small tropical catchment and some management implications. *Applied*  
479 *Geography*, 21(4), 387–412. [https://doi.org/10.1016/S0143-6228\(01\)00013-3](https://doi.org/10.1016/S0143-6228(01)00013-3)
- 480 Collins, A. L., & Walling, D. E. (2002). Selecting fingerprint properties for discriminating potential  
481 suspended sediment sources in river basins. *Journal of Hydrology*, 261, 218–244.  
482 [https://doi.org/10.1016/S0022-1694\(02\)00011-2](https://doi.org/10.1016/S0022-1694(02)00011-2)
- 483 Collins, A. L., Walling, D. E., Webb, L., King, P. (2010). Apportioning catchment scale sediment sources  
484 using a modified composite fingerprinting technique incorporating property weightings and  
485 prior information. *Geoderma*, 155(3–4), 249–261.  
486 <https://doi.org/10.1016/j.geoderma.2009.12.008>
- 487 Collins, A. L., Zhang, Y., McChesney, D., Walling, D. E., Haley, S. M., Smith, P. (2012). Sediment source  
488 tracing in a lowland agricultural catchment in southern England using a modified procedure  
489 combining statistical analysis and numerical modelling. *Science of The Total Environment*, 414,  
490 301–317. <https://doi.org/10.1016/j.scitotenv.2011.10.062>
- 491 Cooper, R. J., Krueger, T., Hiscock, K. M., & Rawlins, B. G. (2014). Sensitivity of fluvial sediment source  
492 apportionment to mixing model assumptions: A Bayesian model comparison. *Water Resources*  
493 *Research*, 50(11), 9031–9047. <https://doi.org/doi:10.1002/2014WR016194>
- 494 Du, P., & Walling, D. E. (2016). Fingerprinting surficial sediment sources: Exploring some potential  
495 problems associated with the spatial variability of source material properties. *Journal of*  
496 *Environmental Management*, 1–12. <https://doi.org/10.1016/j.jenvman.2016.05.066>
- 497 Evrard, O., Navratil, O., Ayrault, S., Ahmadi, M., Némery, J., Legout, C., Esteves, M. (2011). Combining  
498 suspended sediment monitoring and fingerprinting to determine the spatial origin of fine  
499 sediment in a mountainous river catchment. *Earth Surface Processes and Landforms*, 36(8),  
500 1072–1089. <https://doi.org/10.1002/esp.2133>
- 501 Evrard, O., Poulénard, J., Némery, J., Ayrault, S., Gratiot, N., Duvert, C., Esteves, M. (2013). Tracing  
502 sediment sources in a tropical highland catchment of central Mexico by using conventional and  
503 alternative fingerprinting methods. *Hydrological Processes*, 27(6), 911–922.  
504 <https://doi.org/10.1002/hyp.9421>
- 505 Frankl, A., Prêtre, V., Nyssen, J., Salvador, P-G. (2017). The success of recent land management  
506 efforts to reduce soil erosion in northern France. *Geomorphology*, 303, 84–93.  
507 <https://doi.org/10.1016/j.geomorph.2017.11.018>
- 508 Fryirs, K., & Gore, D. (2013). Sediment tracing in the upper Hunter catchment using elemental and  
509 mineralogical compositions: Implications for catchment-scale suspended sediment  
510 (dis)connectivity and management. *Geomorphology*, 193, 112–121.  
511 <https://doi.org/10.1016/j.geomorph.2013.04.010>
- 512 Gellis, A. C., & Walling, D. E. (2011). Sediment Source Fingerprinting (Tracing) and Sediment Budgets  
513 as Tools in Targeting River and Watershed Restoration Programs. *Geophysical Monograph*  
514 *Series*, 194(JANUARY), 263–291. <https://doi.org/10.1029/2010GM000960>



- 515 Gellis, A. C., & Noe, G. B. (2013). Sediment source analysis in the Linganore Creek watershed,  
516 Maryland, USA, using the sediment fingerprinting approach: 2008 to 2010. *Journal of Soils and*  
517 *Sediments*, 13 (10), 1735-1753. <https://doi.org/10.1007/s11368-013-0771-6>
- 518 Gellis, A. C., Noe, G. B., Clune, J. W., Myers, M. K., Hupp, C. R., Schenk, E. R., Schwarz, G. E. (2015).  
519 Sources of the grained sediment in the Linganore Creek watershed, Frederick and Carroll  
520 Counties, Maryland, 2008-10: U.S. Geological Survey Scientific Investigations Report 2014-5147,  
521 56p., <http://dx.doi.org/10.31313/sir20145147>.
- 522 Gorman Sanisaca, L. E., Gellis, A. C., & Lorenz, D. L. (2017). Determining the Sources of Fine-Grained  
523 Sediment Using the Sediment Source Assessment Tool ( Sed \_ SAT ): U.S. Geological Survey  
524 Open File Report 2017-1062, 104 p., <https://doi.org/10.3133/ofr20171062>.
- 525 Guzmán, G., Quinton, J. N., Nearing, M. A., Mabit, L., Gómez, J. A. (2013). Sediment tracers in water  
526 erosion studies: current approaches and challenges. *Journal of Soils and Sediments*, 13(4), 816–  
527 833. <https://doi.org/10.1007/s11368-013-0659-5>
- 528 Haddadchi, A., Ryder, D. S., Evrard, O., Olley, J. (2013). Sediment fingerprinting in fluvial systems:  
529 review of tracers, sediment sources and mixing models. *International Journal of Sediment*  
530 *Research*, 28(4), 560–578. [https://doi.org/10.1016/S1001-6279\(14\)60013-5](https://doi.org/10.1016/S1001-6279(14)60013-5)
- 531 Haddadchi, A., Olley, J. & Laceby, P. (2014). Accuracy of mixing models in predicting sediment source  
532 contributions. *Science of the Total Environment*, 497-498, 139-152.  
533 <https://dx.doi.org/10.1016/j.scitotenv.2014.07.105>
- 534 Haddadchi, A., Olley, J., & Pietsch, T. (2015). Quantifying sources of suspended sediment in three size  
535 fractions. *Journal of Soils and Sediments*, 15(10), 2086-2100. <https://doi.org/10.1007/s11368-015-1196-1>
- 537 Hughes, A. O., Olley, J. M., Croke, J. C., McKergow, L. A. (2009). Sediment sources changes over the  
538 last 250 years in a dry-tropical catchment, central Queensland, Australia. *Geomorphology*,  
539 104(3-4), 262–275. <https://doi.org/10.1016/j.geomorph.2008.09.003>
- 540 Huisman, N. L. H., Karthikeyan, K. G., Lamba, J., Thompson, A. M., Peaslee, G. (2013). Quantification  
541 of seasonal sediment and phosphorus transport dynamics in an agricultural watershed using  
542 radiometric fingerprinting techniques. *Journal of Soils and Sediments*, 13(10), 1724-1734.  
543 <https://doi.org/10.1007/s11368-013-0796-0>
- 544 Kayvantash, D. (2016). *Caractérisation des particules ferrugineuses dans la Seine avec le magnétisme*  
545 *environnemental*. Thèse de doctorat. Université de recherche Paris Sciences et Lettres, France.  
546 268p.
- 547 Kayvantash, D., Cojan, I., Kissel, C., Franke, C. (2017). Magnetic fingerprint of the sediment load in a  
548 meander bend section of the Seine River (France). *Geomorphology*, 286, 14–26.  
549 <https://doi.org/10.1016/j.geomorph.2017.02.020>
- 550 Koiter, A. J., Owens, P. N., Petticrew, E. L., Lobb, D. A. (2013). The behavioural characteristics of  
551 sediment properties and their implications for sediment fingerprinting as an approach for  
552 identifying sediment sources in river basins. *Earth-Science Reviews*, 125, 24–42.  
553 <https://doi.org/10.1016/j.earscirev.2013.05.009>
- 554 Koiter, A. J., Owens, P. N., Petticrew, E. L., Lobb, D. A. (2015). The role of gravel channel beds on the  
555 particle size and organic matter selectivity of transported fine-grained sediment: implications  
556 for sediment fingerprinting and biogeochemical flux research. *Journal of Soils and Sediments*,  
557 15(10), 2174–2188. <https://doi.org/10.1007/s11368-015-1203-6>

- 558 Kraushaar, S., Schumann, T., Ollesch, G., Schubert, M., Vogel, H.-J., Siebert, C. (2015). Sediment  
559 fingerprinting in northern Jordan: element-specific correction factors in a carbonatic setting.  
560 *Journal of Soils and Sediments*, 15(10), 2155–2173. <https://doi.org/10.1007/s11368-015-1179-2>
- 561 Krein, A., Petticrew, E., & Udelhoven, T. (2003). The use of fine sediment fractal dimensions and  
562 colour to determine sediment sources in a small watershed. *Catena*, 53(2), 165–179.  
563 [https://doi.org/10.1016/S0341-8162\(03\)00021-3](https://doi.org/10.1016/S0341-8162(03)00021-3)
- 564 Lacey, J. P., Evrard, O., Smith, H. G., Blake, W. H., Olley, J. M., Minella, J. P. G., Owens, P. N. (2017).  
565 The challenges and opportunities of addressing particle size effects in sediment source  
566 fingerprinting: A review. *Earth-Science Reviews*, 169, 85–103.  
567 <https://doi.org/10.1016/j.earscirev.2017.04.009>
- 568 Lacey, J. P., & Olley, J. (2015). An examination of geochemical modelling approaches to tracing  
569 sediment sources incorporating distribution mixing and elemental correlations. *Hydrological*  
570 *Processes*, 29(6), 1669–1685. <https://doi.org/10.1002/hyp.10287>
- 571 Lamba, J., Karthikeyan, K. G., & Thompson, A. M. (2015). Apportionment of suspended sediment  
572 sources in an agricultural watershed using sediment fingerprinting. *Geoderma*, 239–240, 25–33.  
573 <https://doi.org/10.1016/j.geoderma.2014.09.024>
- 574 Le Gall, M., Evrard, O., Foucher, A., Lacey, J. P., Salvador-Blanes, S., Thil, F., Ayrault, S. (2016).  
575 Quantifying sediment sources in a lowland agricultural catchment pond using <sup>137</sup>Cs activities  
576 and radiogenic <sup>87</sup>Sr/<sup>86</sup>Sr ratios. *Science of the Total Environment*, 566–567, 968–980.  
577 <https://doi.org/10.1016/j.scitotenv.2016.05.093>
- 578 Legout, C., Poulenard, J., Nemery, J., Navratil, O., Grangeon, T., Evrard, O., Esteves, M. (2013).  
579 Quantifying suspended sediment sources during runoff events in headwater catchments using  
580 spectroradiometry. *Journal of Soils and Sediments*, 13(8), 1478–1492.  
581 <https://doi.org/10.1007/s11368-013-0728-9>
- 582 Li, T., Sun, G., Yang, C., Liang, K., Ma, S., Huang, L., Luo, W. (2019). Source apportionment and source-  
583 to-sink transport of major and trace elements in coastal sediments: Combining positive matrix  
584 factorization and sediment trend analysis. *Science of the Total Environment*, 651, 344–356.  
585 <https://doi.org/10.1016/j.scitotenv.2018.09.198>
- 586 Martínez-Carreras, N., Udelhoven, T., Krein, A., Gallart, F., Iffly, J. F., Ziebel, J., Walling, D. E. (2010).  
587 The use of sediment colour measured by diffuse reflectance spectrometry to determine  
588 sediment sources: Application to the Attert River catchment (Luxembourg). *Journal of*  
589 *Hydrology*, 382(1–4), 49–63. <https://doi.org/10.1016/j.jhydrol.2009.12.017>
- 590 Motha, J. A., Wallbrink, P. J., Hairsine, P. B., Grayson, R. B. (2003). Determining the sources of  
591 suspended sediment in a forested catchment in southeastern Australia. *Water Resources*  
592 *Research*, 39(3), 1056. <https://doi.org/10.1029/2001wr000794>
- 593 Motha, J. A., Wallbrink, P. J., Hairsine, P. B., Grayson, R. B. (2004). Unsealed roads as suspended  
594 sediment sources in an agricultural catchment in south-eastern Australia. *Journal of Hydrology*,  
595 286(1–4), 1–18. <https://doi.org/10.1016/j.jhydrol.2003.07.006>
- 596 Nosrati, K., Collins, A. L., & Madankan, M. (2018). Fingerprinting sub-basin spatial sediment sources  
597 using different multivariate statistical techniques and the Modified MixSIR model. *Catena*, 164,  
598 32–43. <https://doi.org/10.1016/j.catena.2018.01.003>
- 599 Palazón, L., Latorre, B., Gaspar, L., Blake, W. H., Smith, H. G., Navas, A. (2015). Comparing catchment  
600 sediment fingerprinting procedures using an auto-evaluation approach with virtual sample

- 601 mixtures. *Science of The Total Environment*, 532, 456–466.  
602 <https://doi.org/10.1016/j.scitotenv.2015.05.003>
- 603 Patault, E. (2018). *Analyse multi-échelle des processus d'érosion hydrique et de transferts*  
604 *sédimentaires en territoire agricole: exemple du bassin versant de la Canche*. Thèse de doctorat.  
605 IMT Lille Douai, France. 300p.
- 606 Phillips, J. M., Russell, M. A., & Walling, D. E. (2000). Time-integrated sampling of fluvial suspended  
607 sediment: a simple methodology for small catchments. *Hydrological Processes*, 14(14), 2589-  
608 2602. [https://doi.org/10.1002/1099-1085\(20001015\)14:14<2589::AID-HYP94>3.0.CO;2-D](https://doi.org/10.1002/1099-1085(20001015)14:14<2589::AID-HYP94>3.0.CO;2-D)
- 609 Poulenard, J., Perrette, Y., Fanget, B., Quetin, P., Trevisan, D., Dorioz, J. M. (2009). Infrared  
610 spectroscopy tracing of sediment sources in a small rural watershed (French Alps). *Science of*  
611 *the Total Environment*, 407(8), 2808–2819. <https://doi.org/10.1016/j.scitotenv.2008.12.049>
- 612 Pulley, S., Foster, I., & Antunes, P. (2015). The application of sediment fingerprinting to floodplain  
613 and lake sediment cores: assumptions and uncertainties evaluated through case studies in the  
614 Nene Basin, UK. *Journal of Soils and Sediments*, 15(10), 2132-2154.  
615 <https://doi.org/10.1007/s11368-015-1136-0>
- 616 Pulley, S. & Collins, A. L. (2018). Tracing catchment fine sediment sources using the new SIFT  
617 (Sediment Fingerprinting Tool) open source software. *Science of the Total Environment*, 635,  
618 838–858. <https://doi.org/10.1016/j.scitotenv.2018.04.126>
- 619 R Core Team (2013). R: A language and environment for statistical computing. R Foundation for  
620 statistical computing, Vienna, Austria. URL: <http://www.R-project.org/>
- 621 Russell, M. A., & Walling, D. E. (2000). Appraisal of a simple sampling device for collecting time-  
622 integrated fluvial suspended sediment samples. *The Role of Erosion and Sediment Transport in*  
623 *Nutrient and Contaminant Transfer (Proceedings of a symposium held at Waterloo, Canada,*  
624 *July 2000)*. IAHS Publ. no. 263.
- 625 Russell, M. A., Walling, D. E., & Hodgkinson, R. . (2001). Suspended sediment sources in two small  
626 lowland agricultural catchments in the UK. *Journal of Hydrology*, 252(1–4), 1–24.  
627 [https://doi.org/10.1016/S0022-1694\(01\)00388-2](https://doi.org/10.1016/S0022-1694(01)00388-2)
- 628 Shapiro, S. S., & Wilk, M. B. (1965). An Analysis of Variance Test for Normality ( Complete Samples ),  
629 52(3), 591–611. Retrieved from <http://www.jstor.org/stable/2333709>
- 630 Sherriff, S. C., Franks, S. W., Rowan, J. S., Fenton, O., Ó'hUallacháin, D. (2015). Uncertainty-based  
631 assessment of tracer selection, tracer non-conservativeness and multiple solutions in sediment  
632 fingerprinting using synthetic and field data. *Journal of Soils and Sediments*, 15(10), 2101-2116.  
633 <https://doi.org/10.1007/s11368-015-1123-5>
- 634 Smith, H. G., Evrard, O., Blake, W. H., Owens, P. N. (2015). Preface—Addressing challenges to  
635 advance sediment fingerprinting research. *Journal of Soils and Sediments*, 15(10), 2033-2037.  
636 <https://doi.org/10.1007/s11368-015-1231-2>
- 637 Tessier, L. (2003). *Transport et caractérisation des matières en suspension dans le bassin versant de la*  
638 *Seine : identification de signatures naturelles et anthropiques*. Thèse de doctorat. Ecole des  
639 Ponts ParisTech.
- 640 Theuring, P., Collins, A. L., & Rode, M. (2015). Source identification of fine-grained suspended  
641 sediment in the Kharaa River basin, northern Mongolia. *Science of The Total Environment*, 526,  
642 77–87. <https://doi.org/10.1016/j.scitotenv.2015.03.134>

- 643 Vale, S. S., Fuller, I. C., Procter, J. N., Basher, L. R., Smith, I. E. (2016). Application of a confluence-  
644 based sediment-fingerprinting approach to a dynamic sedimentary catchment, New Zealand.  
645 *Hydrological Processes*, 30(5), 812–829. <https://doi.org/10.1002/hyp.10611>
- 646 Vale, S. S., Fuller, I. C., Procter, J. N., Basher, L. R., Smith, I. E. (2016). Characterization and  
647 quantification of suspended sediment sources to the Manawatu River, New Zealand. *Science of*  
648 *the Total Environment*, 543, 171-186. <https://doi.org/10.1016/j.scitotenv.2015.11.003>
- 649 Venables, W. N. & Ripley, B. D. (2002). *Modern Applied Statistics With S. Technometrics*.  
650 <https://doi.org/10.1198/tech.2003.s33>
- 651 Walling, D. E., Russell, M. A., Hodgkinson, R. A., Zhang, Y. (2002). Establishing sediment budgets for  
652 two small lowland agricultural catchments in the UK. *Catena*, 47(4), 323–353.  
653 [https://doi.org/10.1016/S0341-8162\(01\)00187-4](https://doi.org/10.1016/S0341-8162(01)00187-4)
- 654 Walling, D. E. & Webb, B. W. (1987). Suspended load in gravel bed-rivers: UK experience, in Thorne,  
655 C. R., Bathurst, J. C. and Hey, R. D. (Eds). *Sediment transportation in Gravel-bed river*. Wiley,  
656 Chichester, pp. 691-723.
- 657 Walling, D. E. & Woodward, J. C. (1992). Use of radiometric fingerprints to derive information on  
658 suspended sediment sources. Erosion and Sediment Transport Monitoring Programmes in River  
659 Basins. (Proceedings Oslo Symposium). In *Erosion and sediment transport Programmes in River*  
660 *Basins* (Vol. 210, pp. 64–153).
- 661 Walling, D. E., Woodward, J. C., & Nicholas, A. P. (1993). A multi-parameter approach to fingerprint  
662 suspended-sediment sources. In *Tracers in Hydrology (Proceeding of the Yokohama Symposium,*  
663 *July 1993)*. IAHS Publ. no, 215.
- 664 Weihs, C., Ligges, U., Luebke, K., Raabe, N. (2005). kLaR: analyzing German business cycles. *Data*  
665 *Analysis and Decision Support*, 335–343. [https://doi.org/10.1007/3-540-28397-8\\_36](https://doi.org/10.1007/3-540-28397-8_36)
- 666 Wilkinson, S. N., Hancock, G. J., Bartley, R., Hawdon, A. A., Keen, R. J. (2013). Using sediment tracing  
667 to assess processes and spatial patterns of erosion in grazed rangelands, Burdekin River basin,  
668 Australia. *Agriculture, Ecosystems and Environment*, 180, 90–102.  
669 <https://doi.org/10.1016/j.agee.2012.02.002>
- 670 Zhang, X. C., & Liu, B. L. (2016). Using multiple composite fingerprints to quantify fine sediment  
671 source contributions: a new direction. *Geoderma*, 268, 108-118.  
672 <https://doi.org/10.1016/j.geoderma.2016.01.031>

## Figures

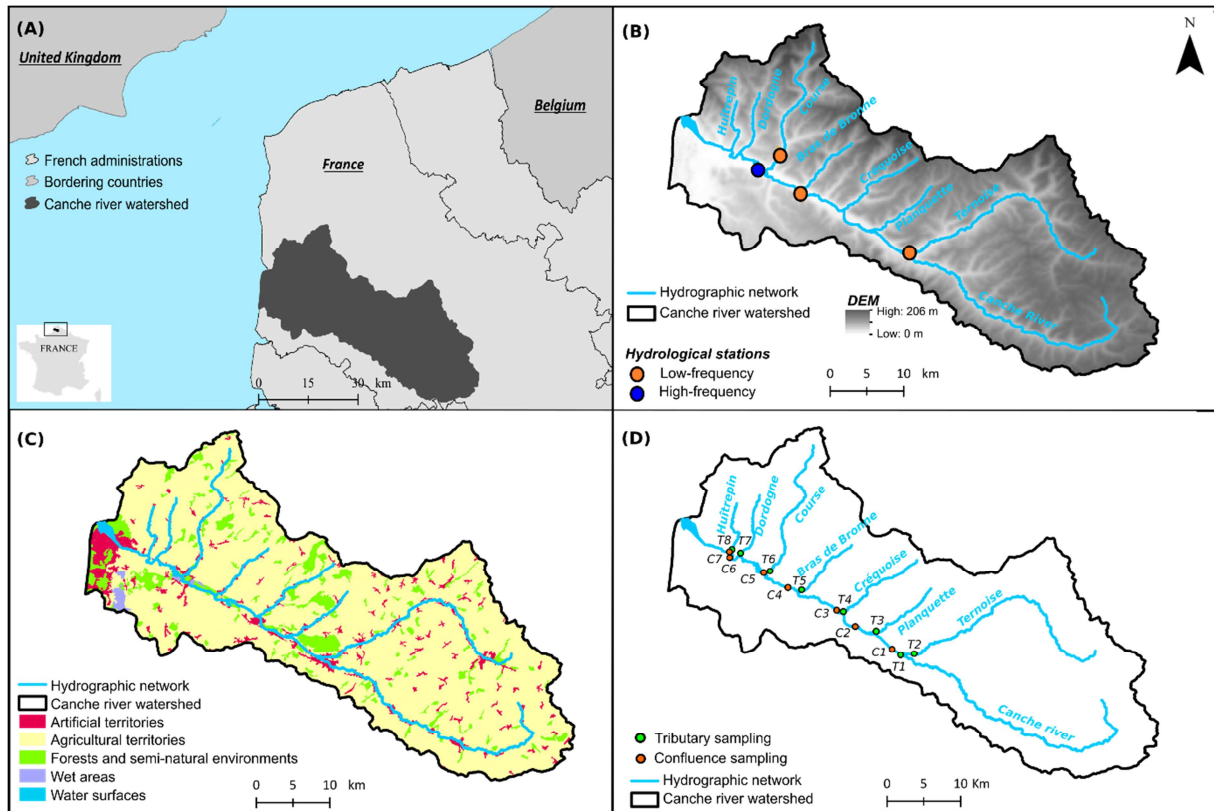


Figure 1 : (A) Overview of the Canche river watershed, (B) Digital elevation model (DEM; m), hydrographic network and location of monitoring stations, (C) Corine Land Cover 2012 and (D) Location of sediment sampling for the study.

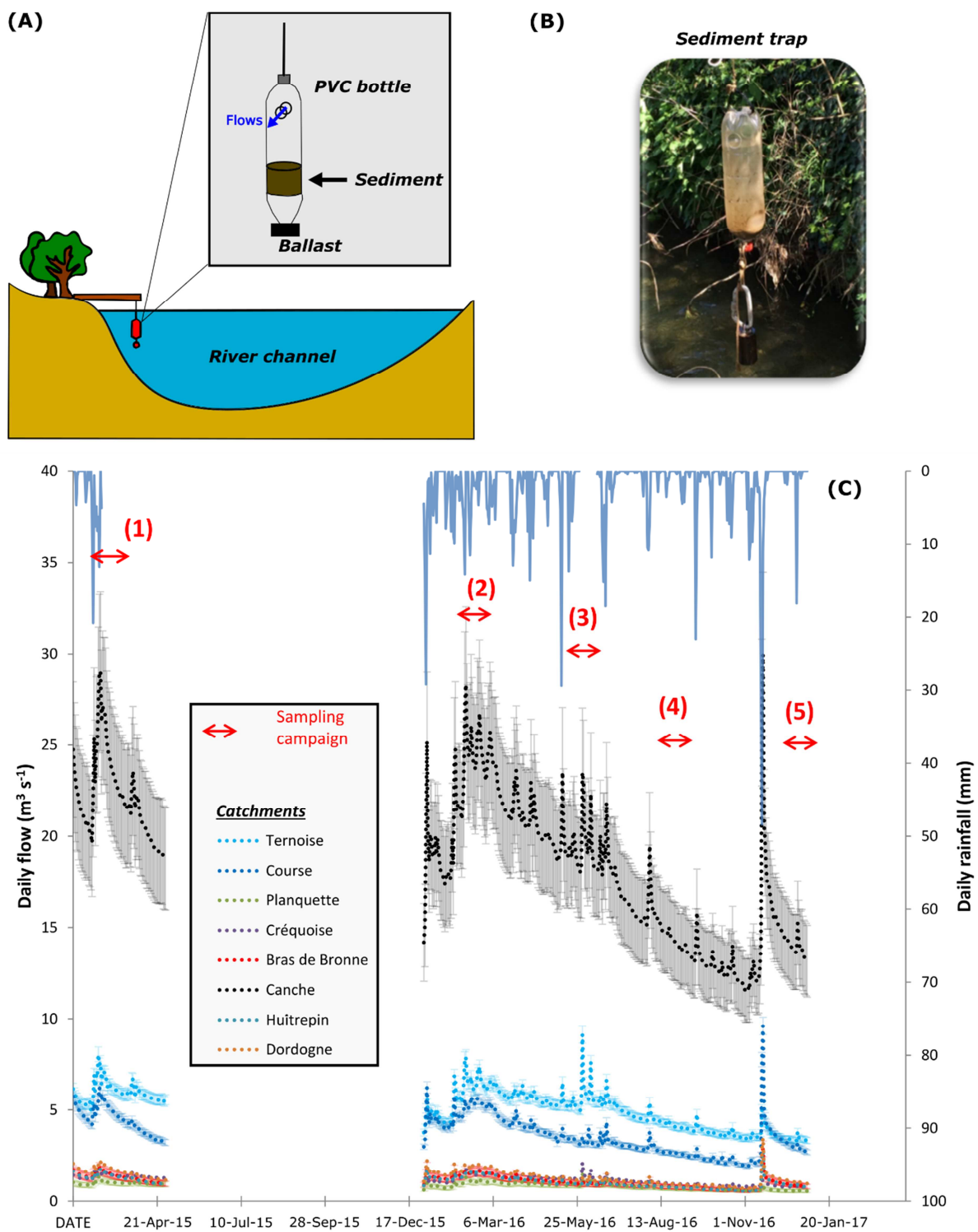


Figure 2 : (A, B) Protocol and experimental device used to sample suspended particulate matter (SPM) for each tributary and confluence in the study, (C) temporal variability of the flow discharge in the Canche river watershed during the five seasonal sampling campaign.

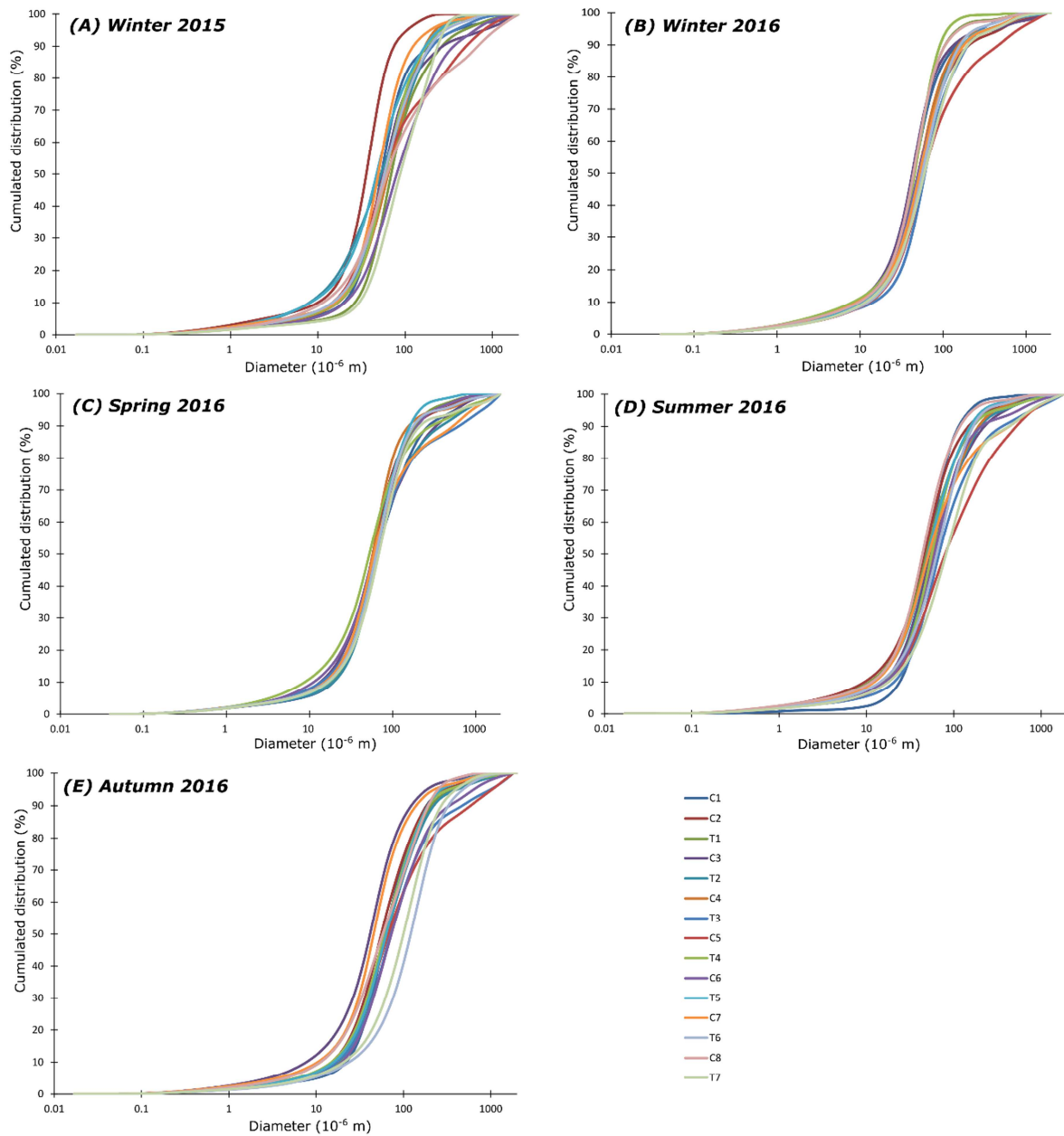


Figure 3: Grain size distribution for all samples collected in the Canche river watershed.

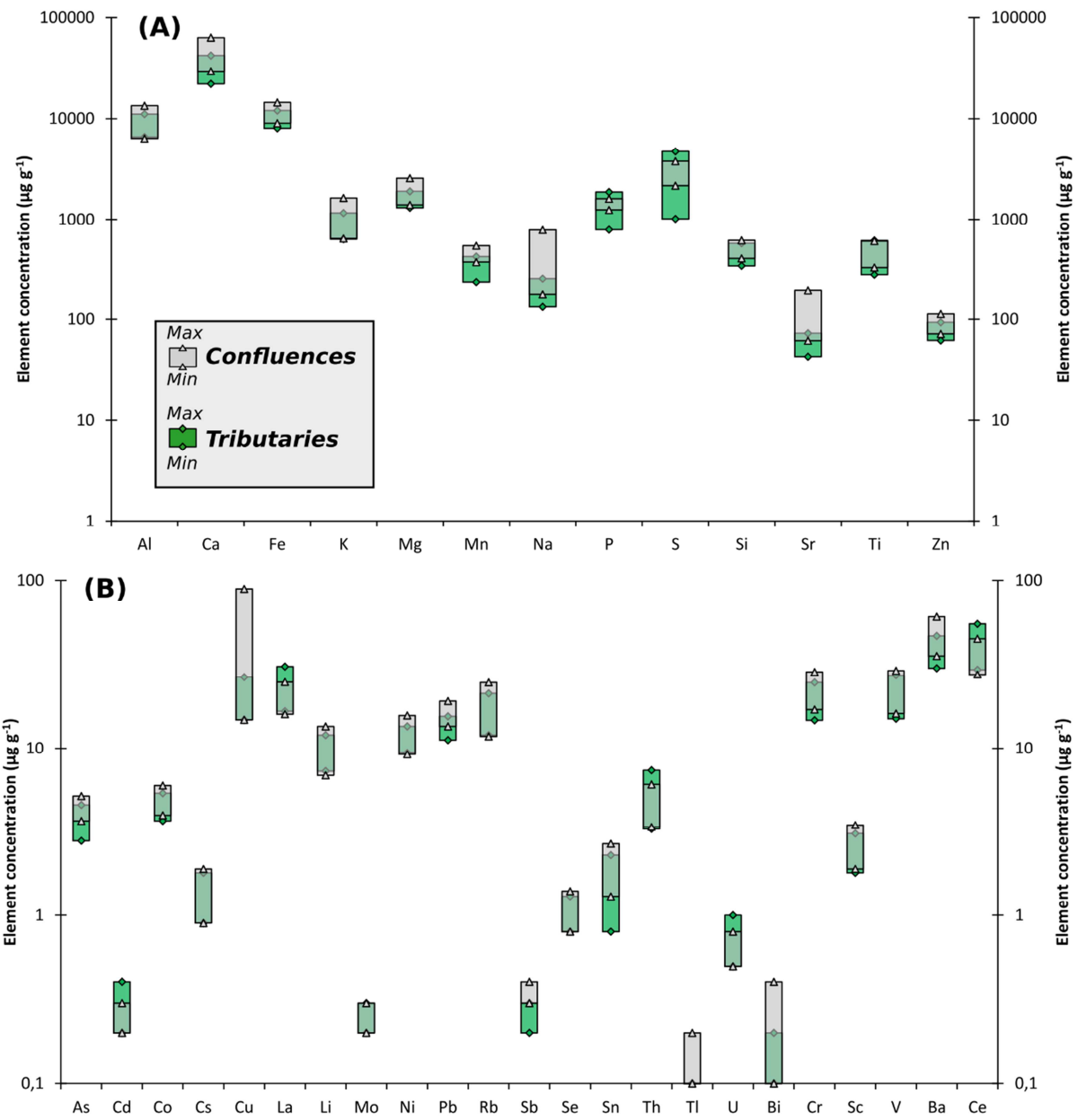


Figure 4: Range of concentrations (expressed in  $\mu\text{g g}^{-1}$ ) of major elements (A) and trace elements (B) in the sediment trap samples during the five seasonal sampling campaigns.



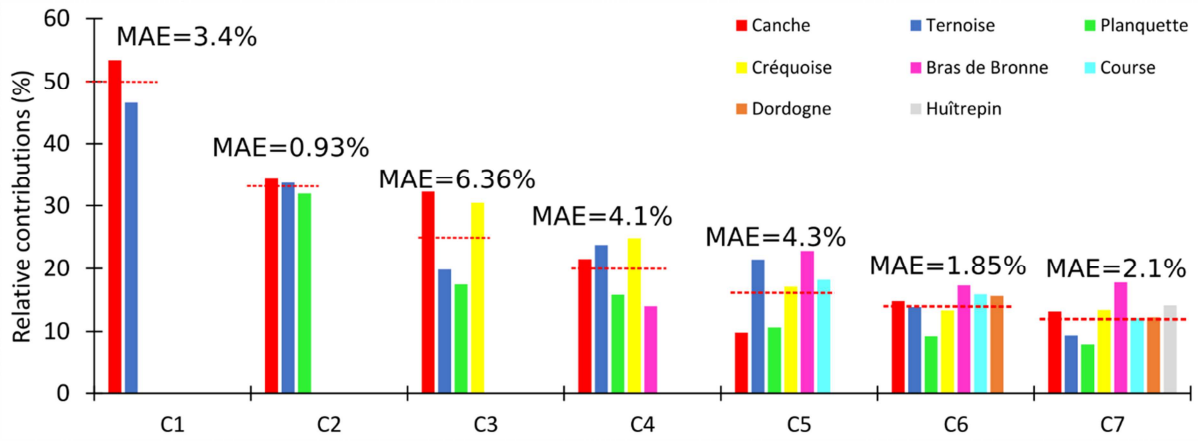


Figure 5 : Mixing model results using virtual mixtures, at each confluences. Red dotted lines indicates the hypothetical contributions (e.g. equal inputs from each tributary). MAE refers to the Mean Absolute Error (%).

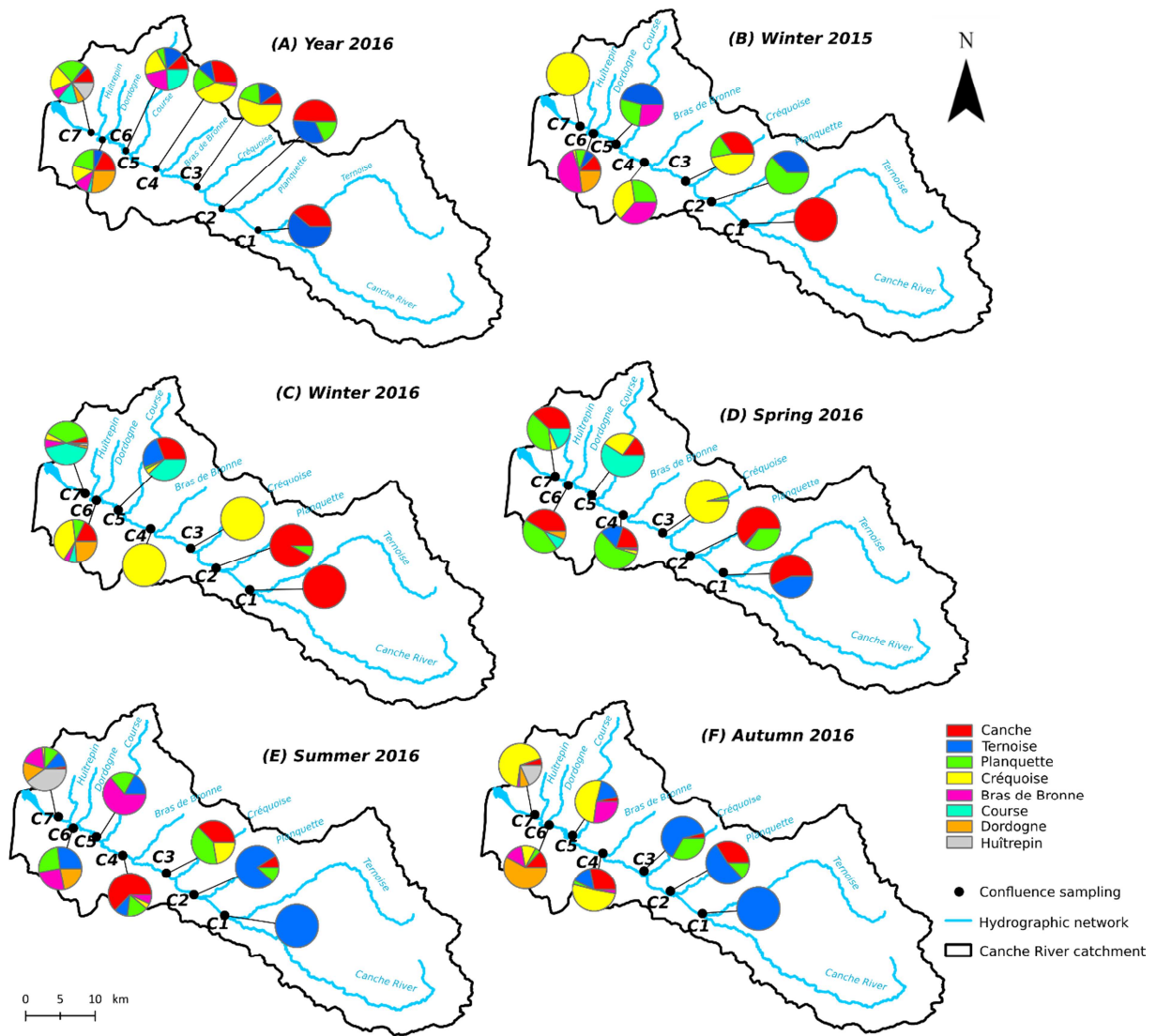


Figure 6 : (A) Annual tributaries relative contributions (%) to the sediment yield in the Canche river watershed and, (B, C, D, E, F) seasonal tributaries relative contributions (%) to the sediment yield in the Canche river watershed.

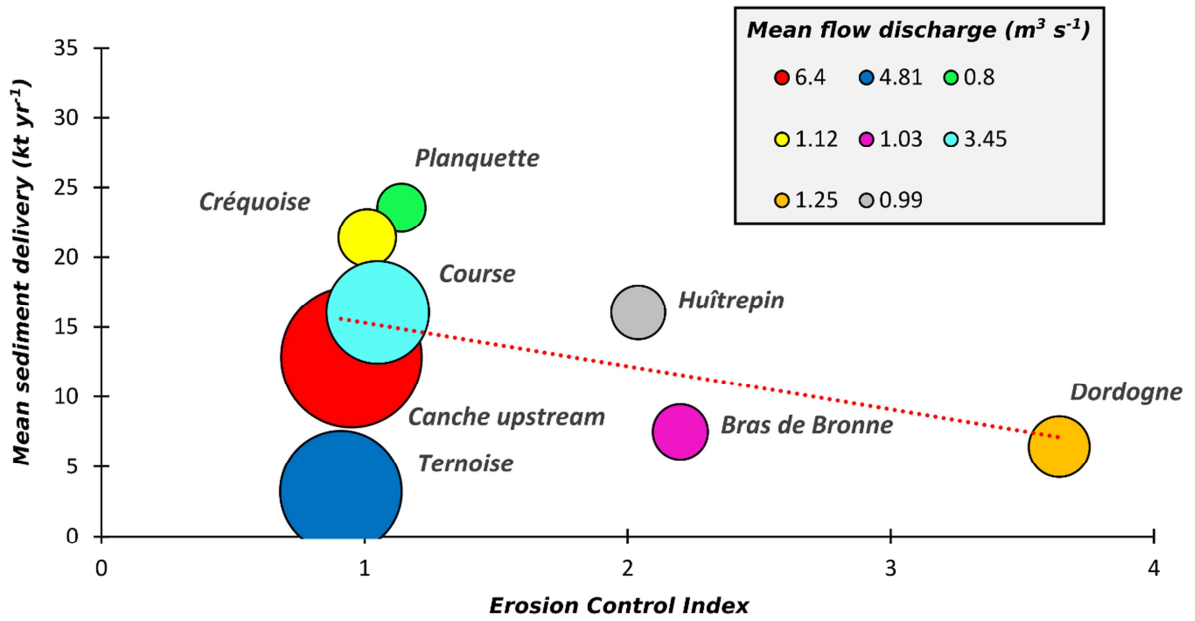


Figure 7: Evaluation of each tributary sediment delivery ( $kt yr^{-1}$ ) as a function of the Erosion Control Index (number of erosion control measures per  $km^2$ ). The bubbles indicates the annual mean flow discharge ( $m^3 s^{-1}$ ). The red dotted line indicates the trend ( $R = 0.41$ ).

## Tables

**Tab. 1: Results of the Bracket test to determine conservative tracers at each confluence.**

Confluence	Conservative tracers
C1	As, Co, La, Mo, Ni, Sn, Th, U, Ce, Al, Ca, Fe, K, Mg, Na, P, S, Sr, Ti, Zn
C2	Cd, La, Sn, Th, U, Ce, Na, Si, Ti
C3	As, Co, Cu, La, Mo, Pb, Sb, Se, Sn, Th, Tl, U, Bi, Cr, V, Ba, Ce, K, Mg, Mn, Na, Si, Sr, Ti, Zn
C4	As, Cd, Co, Cs, La, Li, Pb, Rb, Sb, Sn, Th, Tl, U, Bi, Cr, Sc, V, Ba, Ce, Al, Ca, Fe, K, Mg, Mn, Na, P, S, Si, Sr, Ti, Zn
C5	As, Cd, Co, Cs, Cu, La, Ni, Pb, Rb, Sb, Se, Sn, Th, U, Ba, Ce, Al, Ca, Fe, Mg, Mn, Na, P, S, Si, Sr, Ti, Zn
C6	As, Cd, Co, Cs, Cu, La, Li, Mo, Ni, Pb, Rb, Sb, Se, Sn, Th, Tl, U, Bi, Cr, Sc, V, Ba, Ce, Al, Fe, K, Mn, P, S, Si, Ti, Zn
C7	As, Cd, Co, Cs, La, Li, Mo, Ni, Pb, Rb, Sb, Se, Sn, Th, U, Bi, Cr, V, Ba, Ce, Al, Fe, Mn, P, S, Si, Ti, Zn

**Tab. 2: Results of the stepwise DFA to identify the final composite fingerprint at each confluence.**

C1			C2			C3			C4			C5			C6			C7		
Tracer	% <sup>a</sup>	TDW <sup>b</sup>	Tracer	% <sup>a</sup>	TDW <sup>b</sup>	Tracer	% <sup>a</sup>	TDW <sup>b</sup>	Tracer	% <sup>a</sup>	TDW <sup>b</sup>	Tracer	% <sup>a</sup>	TDW <sup>b</sup>	Tracer	% <sup>a</sup>	TDW <sup>b</sup>	Tracer	% <sup>a</sup>	TDW <sup>b</sup>
Co	60	1.5	La	47	3.5	Bi	44	2.3	Ca	36	3	Ca	34	8.1	Mo	13	2	Mo	14	2.6
Ni	50	1.3	U	40	3	Sr	20	1.1	Bi	30	2.5	Mn	16	3.7	Pb	26	4	Pb	23	4.1
Mg	60	1.5	Na	13	1	Sb	19	1	Mn	19	1.6	Mg	15	3.5	As	16	2.4	As	9	1.6
Ca	40	1	Ti	20	1.5	As	23	1.2	Si	23	1.9	Sb	13	2.9	Se	7	1.1	Se	6	1.1

Total <sup>c</sup>	<b>100</b>	Cd	47	3.5	Se	20	1.1	K	12	1	Si	17	3.9	Ni	6	1	Co	8	1.3
		Si	13	1	Ti	34	1.8	Sb	15	1.3	Cs	13	2.9	Fe	27	4.2	Ni	9	1.6
		Total <sup>c</sup>	<b>53</b>		Total <sup>c</sup>	<b>85</b>		Fe	24	2	Rb	8	1.9	Co	11	1.7	Fe	21	3.8
								Total <sup>c</sup>	<b>69</b>		Sr	14	3.3	P	7	1.1	Mn	12	2.1
											Na	4	1	Mn	14	2.1	Zn	8	1.3
											P	8	1.9	Zn	9	1.3	Cs	9	1.7
											As	12	2.7	Total <sup>c</sup>	<b>54</b>		Al	11	1.9
											Ni	8	1.7				Cd	6	1
											Cd	8	1.7				Cr	18	3.1
											Total <sup>c</sup>	<b>62</b>					Total <sup>c</sup>	<b>58</b>	

<sup>a</sup> % source type samples correctly classified by the tracer.

<sup>b</sup> tracer discriminatory weighting used in the mass balance modelling.

<sup>c</sup> % source type samples classified correctly by the final composite fingerprint.

Graphical abstract

